2017 International Conference on Rehabilitation Robotics (ICORR)
QEII Centre, London, UK, July 17-20, 2017.

Exploiting Kinematic Constraints to Compensate Magnetic Disturbances when Calculating Joint Angles of Approximate Hinge Joints from Orientation Estimates of Inertial Sensors*

Daniel Laidig[1], Thomas Schauer[1] and Thomas Seel[1]

***Abstract*— Inertial Measurement Units (IMUs) have become a widely used tool for rehabilitation and other application domains in which human motion is analyzed using an ambulatory or wearable setup. Since the magnetic field is inhomogeneous in indoor environments and in the proximity of ferromagnetic material, standard orientation estimation and joint angle calculation algorithms often lead to inaccurate or even completely wrong results. One approach to circumvent this is to exploit the kinematic constraint that is induced by mechanical hinge joints and also by approximate hinge joints such as the knee joint and the finger (interphalangeal) joints of the human body. We propose a quaternion-based method for joint angle measurement for approximate hinge joints moving through inhomogeneous magnetic fields. The method exploits the kinematic constraint to compensate the error that the magnetic disturbances induce in the IMU orientation estimates. This is achieved by realtime estimation and correction of the relative heading (azimuth) error that is caused by the disturbance. Since the kinematic constraint does not allow heading correction when the joint axis is vertical, we extend the proposed method such that it improves accuracy and robustness when the joint is close to that singularity. We evaluate the method by simulations of a quick hand motion and study the effect of inaccurate sensor-to-segment (anatomical) calibration and joint constraint relaxations. As a main result, the proposed method is found to reduce the root-mean-square error of the joint angle from 25.8° to 2.6° in the presence of large magnetic disturbances.**

I. INTRODUCTION

In rehabilitation, Inertial Measurement Units (IMUs) are often used to analyze the motion of human body segments or robotic actuators, cf. Fig. 1. Modern IMUs are equipped with on-board sensor fusion and provide measurements of their orientation with respect to a fixed inertial frame, e.g. in form of a unit quaternion [1]. In order to measure joint angles, an IMU is attached to each of the two body segments forming the joint. Then, an anatomical calibration (sensor-to-segment calibration) is performed in order to determine the relation between sensor axes and segment or joint axes. With this information, segment orientations and then joint angles can be calculated.

One major challenge in the application of IMUs is that the magnetic field is known to be inhomogeneous in indoor environments [2] and near ferromagnetic materials or electronic devices. These disturbances severely limit the accuracy of the measured joint angles in two ways: On the one hand, the sensor orientation estimates are deteriorated, even if recent algorithms manage to leave the inclination part unaffected [3]. On the other hand, magnetic disturbances may also limit the accuracy of the sensor-to-segment calibration.

One way to mitigate or even eliminate these effects is to employ kinematic constraints of the joint. The fact that a hinge has only one rotational degree of freedom has previously been exploited for sensor-to-segment calibration [6] and for joint angle calculation [4], [7]–[9]. This has been achieved by calculating the joint angle directly from orientations with uncertain heading [7], by using Kalman

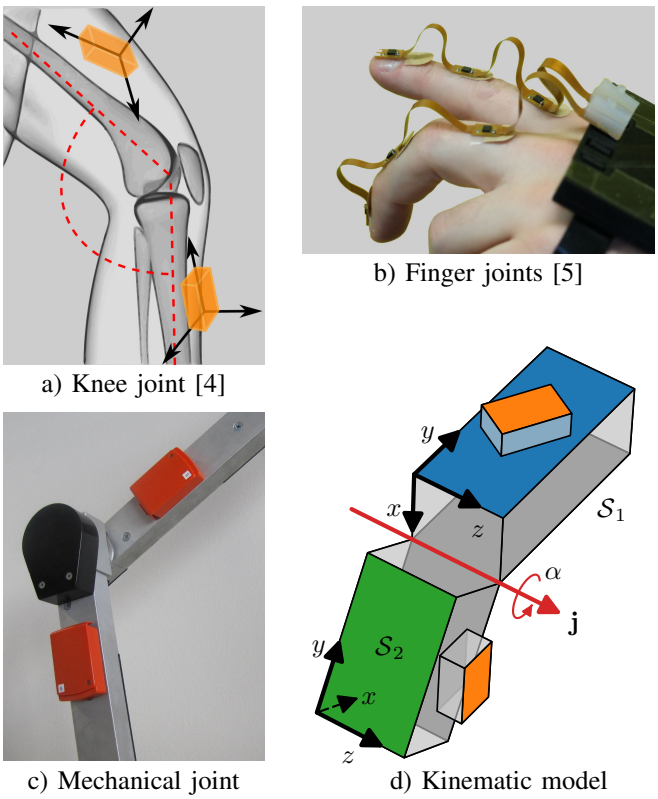

a) Knee joint [4]
b) Finger joints [5]
c) Mechanical joint
d) Kinematic model

Fig. 1. Examples of IMU motion analysis for approximate hinge joints and kinematic model of the joint with the joint axis **j** and coordinate systems (black axes) of segments $\mathcal{S}_1$ and $\mathcal{S}_2$.

*This work has been conducted in the project BeMobil, which is supported by the German Federal Ministry of Research and Education (FKZ 16SV7069K).

[1]Daniel Laidig, Thomas Schauer and Thomas Seel are with Control Systems Group, Technische Universität Berlin, Einsteinufer 17 EN11, 10587 Berlin, Germany
{laidig,schauer,seel}@control.tu-berlin.de

filters [8], by optimization [9] or by complementary filters [4]. However, two aspects have received little attention: Due to a singularity, the kinematic constraint cannot always be used to calculate the joint angle. In case of uncertain sensor-to-segment alignment or imperfect joints, applying the joint constraint induces errors in the obtained joint angle.

In the present contribution, we consider the task of IMU-based joint angle measurements on approximate hinge joints moving in inhomogeneous magnetic fields. Specifically, we introduce a quaternion-based method that uses the hinge joint constraint to determine and correct the error in heading (azimuth) caused by magnetic disturbance. Unlike previous methods, we propose a filter for singularity treatment. Using simulations, we test the performance of this method in homogenous and heavily disturbed magnetic fields and investigate the sensitivity to the joint not being a perfect hinge joint and to errors in sensor-to-segment calibration.

II. METHOD

Consider a hinge joint with one IMU on each segment. The joint moves freely in three-dimensional space. Each IMU performs sensor fusion to determine its orientation with respect to a fixed inertial frame. Furthermore, assume that the sensor-to-segment orientations have been identified, e.g. from arbitrary motions of the joint using the methods in [6]. Thus, we are given two quaternions ${}^{\mathcal{S}1}_{\mathcal{E}}\mathbf{q}$ and ${}^{\mathcal{S}2}_{\mathcal{E}}\mathbf{q}$ describing the orientations of the two body segments $\mathcal{S}_1$ and $\mathcal{S}_2$ relative to a common fixed inertial frame $\mathcal{E}$.

Denote the coordinates of the hinge joint axis in the coordinate system of $\mathcal{S}_1$ by $\mathbf{j}_1$ and the coordinates of the hinge joint axis in the coordinate system of $\mathcal{S}_2$ by $\mathbf{j}_2$. Note that $\mathbf{j}_1$ and $\mathbf{j}_2$ do not change when the joint moves. Furthermore, transformed to the fixed inertial frame $\mathcal{E}$, $\mathbf{j}_1$ and $\mathbf{j}_2$ have the same coordinates, i.e.

$$ {}^{\mathcal{S}1}_{\mathcal{E}}\mathbf{q} \otimes \mathbf{j}_1 \otimes {}^{\mathcal{S}1}_{\mathcal{E}}\mathbf{q}^{-1} = {}^{\mathcal{S}2}_{\mathcal{E}}\mathbf{q} \otimes \mathbf{j}_2 \otimes {}^{\mathcal{S}2}_{\mathcal{E}}\mathbf{q}^{-1} \tag{1} $$

holds for all times[1].

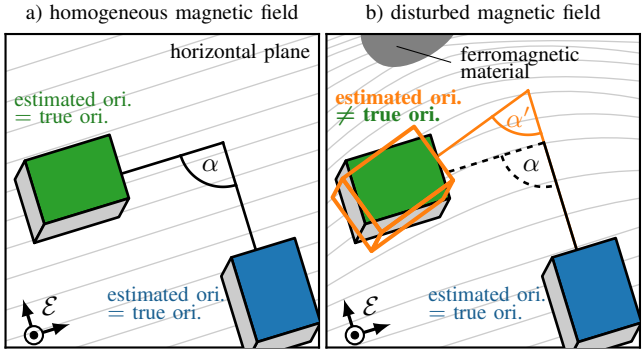

Fig. 2. The orientation of two bodies is estimated in a homogeneous magnetic field and in a magnetic field disturbed by a ferromagnetic material. The magnetic disturbance causes the estimated relative orientation of the two bodies to be corrupted, i.e. we obtain wrong joint angles.

[1]We use $\otimes$ to denote quaternion multiplication. When three-dimensional vectors $\mathbf{v} \in \mathbb{R}^3$ are multiplied with quaternions, we implicitly regard them as their corresponding pure quaternions $[\,0 \;\; \mathbf{v}^{\mathrm{T}}\,]^{\mathrm{T}}$.

However, this is only true if the magnetic field is homogeneous. When magnetic disturbances occur, the IMU can no longer determine its true orientation, since accelerometer and magnetometer readings are required to compensate integration drift effects that are due to gyroscope bias. Previously, it has been suggested to use adaptive sensor fusion weights and disregard the magnetometer readings if disturbances occur. This approach has two drawbacks: On the one hand, it is often difficult to detect that the measurement is disturbed – especially if the disturbance does not affect the norm of the measured field vector. On the other hand, pure integration of the gyroscope while neglecting the magnetometer reading will work only for the trivial case of quickly vanishing disturbances. Since gyroscope biases are often in the range of $1\frac{^\circ}{s}$, integration errors will quickly become unacceptably large.

We therefore consider the non-trivial case in which the magnetic field remains inhomogeneous for at least ten seconds and thus the sensor orientation estimates are affected regardless of the sensor fusion. When the sensor fusion algorithm of an IMU uses disturbed magnetometer data, then the inclination (roll and pitch) and the heading (yaw, azimuth) portion of the orientation are typically affected. However, it was demonstrated recently that sensor fusion can be carried out in a way that assures accurate inclination even in severely disturbed magnetic fields [3].

We assume that such an algorithm is employed and therefore only the heading portions of the estimated segment orientations become inaccurate, c.f. Fig. 2. Due to these heading errors, the measured segment orientations ${}^{\mathcal{S}1}_{\mathcal{E}1}\mathbf{q}$ and ${}^{\mathcal{S}2}_{\mathcal{E}2}\mathbf{q}$ do no longer describe the orientation of the segments with respect to a common fixed frame but with respect to two reference frames $\mathcal{E}_1$ and $\mathcal{E}_2$ that are shifted[2] by a rotation around the vertical axis:

$$ {}^{\mathcal{S}1}_{\mathcal{E}}\mathbf{q} = {}^{\mathcal{E}1}_{\mathcal{E}}\mathbf{q} \otimes {}^{\mathcal{S}1}_{\mathcal{E}1}\mathbf{q}, \tag{2} $$

$$ {}^{\mathcal{S}2}_{\mathcal{E}}\mathbf{q} = {}^{\mathcal{E}2}_{\mathcal{E}}\mathbf{q} \otimes {}^{\mathcal{S}2}_{\mathcal{E}2}\mathbf{q}. \tag{3} $$

In the unrealistic case that both orientation estimates are affected in exactly the same way, $\mathcal{E}_1$ and $\mathcal{E}_2$ coincide. In general, however, the relative orientation ${}^{\mathcal{S}2}_{\mathcal{S}1}\mathbf{q} = {}^{\mathcal{S}1}_{\mathcal{E}}\mathbf{q}^{-1} \otimes {}^{\mathcal{S}2}_{\mathcal{E}}\mathbf{q}$ between the first and second segment can only be calculated if the rotation between $\mathcal{E}_1$ and $\mathcal{E}_2$ is known:

$$ \begin{aligned} {}^{\mathcal{S}2}_{\mathcal{S}1}\mathbf{q} &= ({}^{\mathcal{E}1}_{\mathcal{E}}\mathbf{q} \otimes {}^{\mathcal{S}1}_{\mathcal{E}1}\mathbf{q})^{-1} \otimes {}^{\mathcal{E}2}_{\mathcal{E}}\mathbf{q} \otimes {}^{\mathcal{S}2}_{\mathcal{E}2}\mathbf{q} \\ &= {}^{\mathcal{S}1}_{\mathcal{E}1}\mathbf{q}^{-1} \otimes \underbrace{{}^{\mathcal{E}1}_{\mathcal{E}}\mathbf{q}^{-1} \otimes {}^{\mathcal{E}2}_{\mathcal{E}}\mathbf{q}}_{=:\, {}^{\mathcal{E}2}_{\mathcal{E}1}\mathbf{q}} \otimes {}^{\mathcal{S}2}_{\mathcal{E}2}\mathbf{q} \end{aligned} \tag{4} $$

where ${}^{\mathcal{E}2}_{\mathcal{E}1}\mathbf{q}$ represents the combined effect of both disturbances and corresponds to a rotation around the global z-axis:

$$ {}^{\mathcal{E}2}_{\mathcal{E}1}\mathbf{q} = \left[\cos\left(\tfrac{\delta}{2}\right) \quad 0 \quad 0 \quad \sin\left(\tfrac{\delta}{2}\right)\right]^{\mathrm{T}}, \tag{5} $$

with $\delta(t)$ being the heading error of ${}^{\mathcal{S}2}_{\mathcal{S}1}\mathbf{q}$ that is caused by the magnetic disturbance. In order to determine the correct relative orientation ${}^{\mathcal{S}2}_{\mathcal{S}1}\mathbf{q}$ and then calculate accurate joint angles, the error $\delta(t)$ must be determined and compensated.

[2]with respect to the ideal common fixed frame $\mathcal{E}$

A. Determining the Heading Error

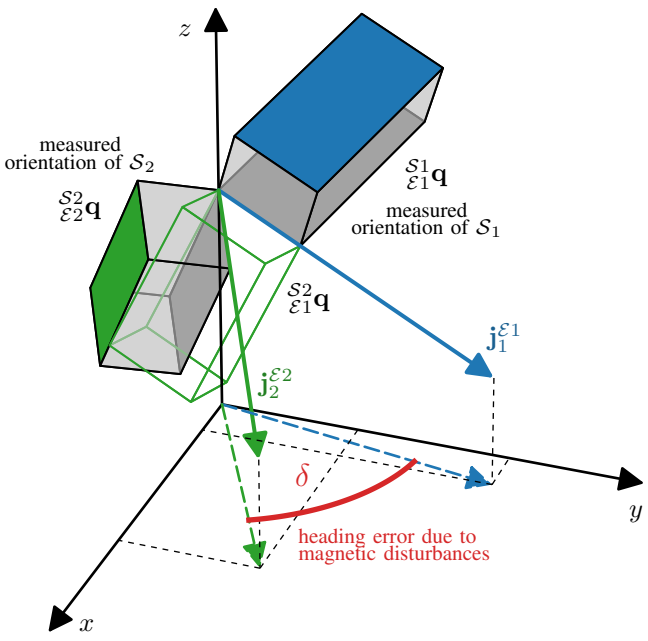

Fig. 3. Two segments $\mathcal{S}_1$ and $\mathcal{S}_2$ are connected by a hinge joint. Due to magnetic disturbances, the measured orientations are subject to the heading error δ. This heading error can be obtained from the projections of the joint axes into the global x-y-plane.

We can determine the difference in the heading of the reference frames as follows. First, we transform the coordinates of the local joint axis vectors of both segments into their respective earth frames:

$$\mathbf{j}_1^{\mathcal{E}1} = {}^{\mathcal{S}1}_{\mathcal{E}1}\mathbf{q} \otimes \mathbf{j}_1 \otimes {}^{\mathcal{S}1}_{\mathcal{E}1}\mathbf{q}^{-1} =: [\, j_{1x} \;\; j_{1y} \;\; j_{1z} \,]^{\mathrm{T}} \tag{6}$$

$$\mathbf{j}_2^{\mathcal{E}2} = {}^{\mathcal{S}2}_{\mathcal{E}2}\mathbf{q} \otimes \mathbf{j}_2 \otimes {}^{\mathcal{S}2}_{\mathcal{E}2}\mathbf{q}^{-1} =: [\, j_{2x} \;\; j_{2y} \;\; j_{2z} \,]^{\mathrm{T}}. \tag{7}$$

We project those vectors in the x-y-plane, i.e. we set j_{1z} and j_{2z} to zero. Then, the heading error δ is given by the difference of the angles of the projected vectors in the x-y-plane, i.e.

$$\delta = \operatorname{atan2}\left(j_{2y},\, j_{2x}\right) - \operatorname{atan2}\left(j_{1y},\, j_{1x}\right). \tag{8}$$

See Fig. 3 for a graphical illustration of this approach.

B. Heading Correction and Joint Angle Calculation

From $\delta(t)$, we calculate ${}^{\mathcal{E}2}_{\mathcal{E}1}\mathbf{q}(t)$ and obtain the segment orientations in a common reference frame[3], e.g.

$${}^{\mathcal{S}2}_{\mathcal{E}1}\mathbf{q} = {}^{\mathcal{E}2}_{\mathcal{E}1}\mathbf{q} \otimes {}^{\mathcal{S}2}_{\mathcal{E}2}\mathbf{q}, \tag{9}$$

which allows us to obtain the relative orientation of one segment with respect to the other, i.e. the joint orientation

$${}^{\mathcal{S}2}_{\mathcal{S}1}\mathbf{q} = {}^{\mathcal{S}1}_{\mathcal{E}1}\mathbf{q}^{-1} \otimes {}^{\mathcal{S}2}_{\mathcal{E}1}\mathbf{q} =: [\, q_w \;\; q_x \;\; q_y \;\; q_z \,]^{\mathrm{T}}. \tag{10}$$

[3]Note that any common reference frame will work, i.e. instead of adjusting the orientation of $\mathcal{S}_2$, we can also bring $\mathcal{S}_1$ to $\mathcal{E}_2$.

We then calculate the joint angle from the joint orientation quaternion. Without loss of generality, the segment coordinate systems are defined so that the joint axis is the local z-axis, i.e. $\mathbf{j}_1 = \mathbf{j}_2 = [\,0 \;\; 0 \;\; 1\,]^{\mathrm{T}}$. One option is to calculate Euler angles and discard the two angles which are assumed to be zero. Using z-x'-y'' Euler angles, as recommended by the International Society of Biomechanics (ISB) for the interphalangeal (finger) joints [10], the angle around the z-axis can be obtained from ${}^{\mathcal{S}2}_{\mathcal{S}1}\mathbf{q}$ as

$$\alpha = \operatorname{atan2}(2q_zq_w - 2q_yq_x,\, q_w^2 + q_y^2 - q_x^2 - q_z^2). \tag{11}$$

Alternatively, we can split the joint orientation into a rotation around the z-axis and a residual quaternion, i.e.

$${}^{\mathcal{S}2}_{\mathcal{S}1}\mathbf{q} = \left[\cos\left(\tfrac{\alpha}{2}\right) \quad 0 \quad 0 \quad \sin\left(\tfrac{\alpha}{2}\right)\right]^{\mathrm{T}} \otimes \mathbf{q}_{\mathrm{res}}. \tag{12}$$

Then, the joint angle α that minimizes the rotation angle[4] of the residual quaternion $\mathbf{q}_{\mathrm{res}}$ is given by

$$\alpha = 2\operatorname{atan2}(q_z,\, q_w). \tag{13}$$

In the remainder of the contribution we employ (13) to calculate the joint angle.

C. Singularity Treatment

When the segments are orientated so that the joint axis is vertical, it is impossible to differentiate between joint rotation and heading errors induced by magnetic disturbances or integration drift. In this case the kinematic constraint becomes useless and δ cannot be calculated, since the horizontal projections of the joint axes become zero.

To mute the correction during time periods with vertical join axis, we design a filter that gives small trust to new values of the heading error $\delta(t)$ when the joint axis is almost vertical and large trust when being far from this singularity.

Assume that δ_k is calculated according to (8) at a fixed rate $f_{\mathrm{s}} = t_{\mathrm{s}}^{-1}$ where k denotes the sampling index.

At each sampling instant, we determine the Euclidean norms of the horizontal projections of the joint axes (dashed errors in Fig. 3) and use the smaller value as the trust rating

$$r_k := \min(\|[\, j_{1x} \;\; j_{1y} \,]^{\mathrm{T}}\|, \|[\, j_{2x} \;\; j_{2y} \,]^{\mathrm{T}}\|). \tag{14}$$

The filtered heading error $\delta_{\mathrm{f},k}$ is obtained with an extended version of an exponential weighted moving average, starting with $\delta_{\mathrm{f},0} = \delta_0$.

$$\delta_{\mathrm{f},k} = \delta_{\mathrm{f},k-1} + r_k \left(1 - e^{-\frac{t_{\mathrm{s}}}{0.05\,\mathrm{s}}}\right) \operatorname{clip}(\delta_k - \delta_{\mathrm{f},k-1}), \tag{15}$$

where the clip function limits the angle difference to $\pm 0.2\,\mathrm{rad}$ and therefore restrains the filter from following quick changes, which may occur close to the singularity.

[4]Minimizing the rotation angle of a quaternion $\mathbf{q}$ is equivalent to maximizing the (absolute value of) the scalar part of $\mathbf{q}$.

III. VALIDATION

To evaluate the proposed method, we perform a validation study in which we simulate an approximate hinge joint that moves through an experimentally determined inhomogeneous magnetic field. Unlike an experimental evaluation with optical motion capture as reference, this approach has the advantage of perfect repeatability and perfectly known reference values (i.e. without measurement errors of a reference system). Furthermore, it allows us to investigate the effect of an imprecise sensor-to-segment calibration and of the joint not being a perfect hinge joint.

A. Simulation

We simulate the motion of two segments, each with an IMU attached centrally, and both connected by an approximate hinge joint. The motion and segment sizes are chosen to mimic a fast three-dimensional motion of a finger (interphalangeal) joint with a duration of $22\,\mathrm{s}$. To obtain a challenging example, the movement is chosen to excite all translatory and rotational degrees of freedom and to avoid any periods of translational or rotational rest.

In light of our discussion in Section II-C, we choose the motion such that the inclination of the joint axis is close to $90°$, i.e. vertical, for several periods of time throughout the course of the motion. See Fig. 4 for an illustration of the movement and [11] for a video animation.

The simulation consists of the following steps (cf. Fig. 5):

1) We calculate IMU raw measurement data (acceleration, angular rate and magnetic field) at $f_\mathrm{s} = 100\,\mathrm{Hz}$ using a realistic measurement model that includes noise on all measurements and a randomized time-variant bias for the gyroscope.
2) We estimate the segment orientation using the algorithm described in [3].
3) We calculate joint angles, once without and once with the proposed heading correction.

Two scenarios are considered. The undisturbed scenario is based on a perfectly homogeneous magnetic field. In addition to this unrealistic case, we consider a magnetic disturbance that was determined experimentally by moving an IMU in the proximity of ferromagnetic metal plates. A marker-based optical motion capture system was used as a reference to allow extraction of the disturbance from the magnetometer readings. Under the disturbance, both dip angle and heading of the magnetic field vector varied by about $100°$.

B. Segment and Motion Dimensions

To assure that the results are not limited to the case of small body segments, we repeat all simulations for segment dimensions and movement space dimensions that are ten times larger than the initially used finger segment dimensions. The segment lengths are increased from about $4\,\mathrm{cm}$ to about $40\,\mathrm{cm}$ and the horizontal distance traveled is increased from about $1\,\mathrm{m}$ to about $10\,\mathrm{m}$, which leads to much larger accelerations. Thereby, the simulated motion is changed to resemble a quick acrobatic motion of a human knee.

C. Results

We perform the described simulation with and without the magnetic disturbance and calculate joint angles with and without the proposed correction. To account for noise, we perform 100 simulation runs for each case. First, consider a perfect sensor-to-segment calibration and a perfect hinge joint. For this case, the obtained root-mean-square errors (RMSE) are given in Table I.

TABLE I
RMSE (MEAN AND STANDARD DEVIATION) FOR DIFFERENT PARAMETER COMBINATIONS

	Disturbance Off	Disturbance On
Correction Off	$0.94°\pm0.30°$	$\mathbf{25.77}°\pm0.30°$
Correction On	$1.14°\pm0.31°$	$\mathbf{2.62}°\pm0.22°$

When the disturbance is not applied, the obtained joint angle estimates are found to have a RMSE of about $1°$, which is in the same range as accuracies reported for similar experimental studies [4] and thus verifies that the IMU measurement model is sufficiently realistic.

Comparing "Correction On/Off" without the simulated disturbance shows that the heading correction only marginally increases the error. Much more significantly, the magnetic disturbance leads to large errors in the uncorrected joint angles and clearly lower errors in the corrected angles.

For the highlighted numbers, which indicate the errors with enabled magnetic disturbance, one typical corresponding angle-over-time plot is given in Fig. 6. The figure also shows the estimated heading error before (δ_est) and after ($\delta_\mathrm{est,f}$) filtering, as well as the true value δ_true.

The magnetic disturbance causes a heading error of up to $90°$ in the estimated orientations, which leads to very large errors in the uncorrected joint angles ($26.0°$ RMSE). The joint axis is almost vertical for five time periods (marked by orange bars), including sampling instants in which it is perfectly vertical. During those periods, the estimated heading error δ_est fluctuates notably. The filter manages to limit the deviation due to the singularity while tracking the calculated heading error closely at other times. With the filtered heading error, we obtain joint angles with a considerably lower error ($2.6°$ RMSE) compared to the uncorrected angles ($26.0°$ RMSE).

D. Sensitivity to Joint and Attachment Errors

We now investigate how sensitive the heading-corrected angles are when we simulate an error in the IMU attachment and allow for small joint rotations around other axes.

a) Sensor-to-segment error: In practice, the accuracy of the sensor-to-segment calibration may vary depending on the employed calibration method. With the parameter E_S, we model the fact that the sensor-to-segment orientations are not precisely known, for example due to inaccurate anatomical calibration or because the sensors slipped after

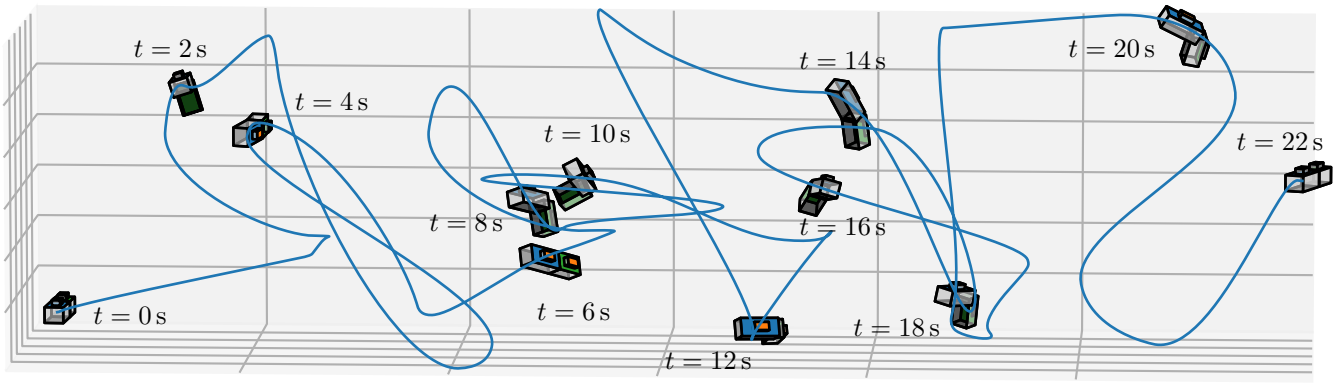

Fig. 4. 3D visualization of the reference movement. See [11] for a video animation.

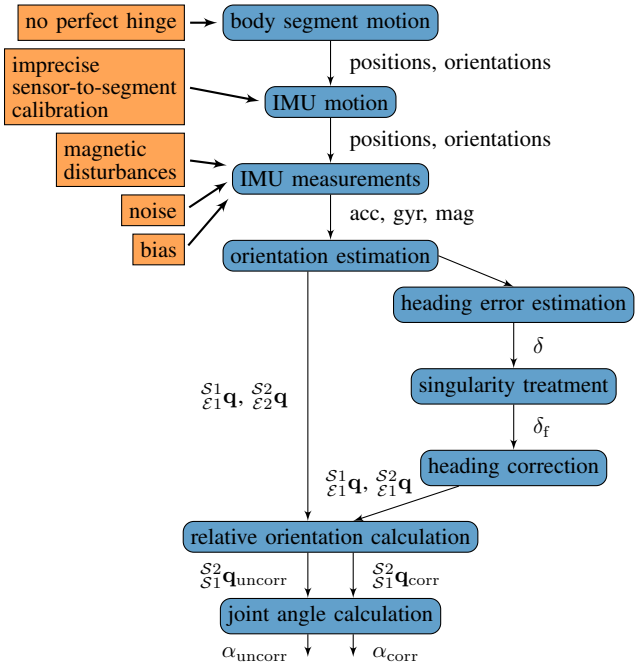

Fig. 5. Overview of the data processing steps and the error sources considered in the simulation study.

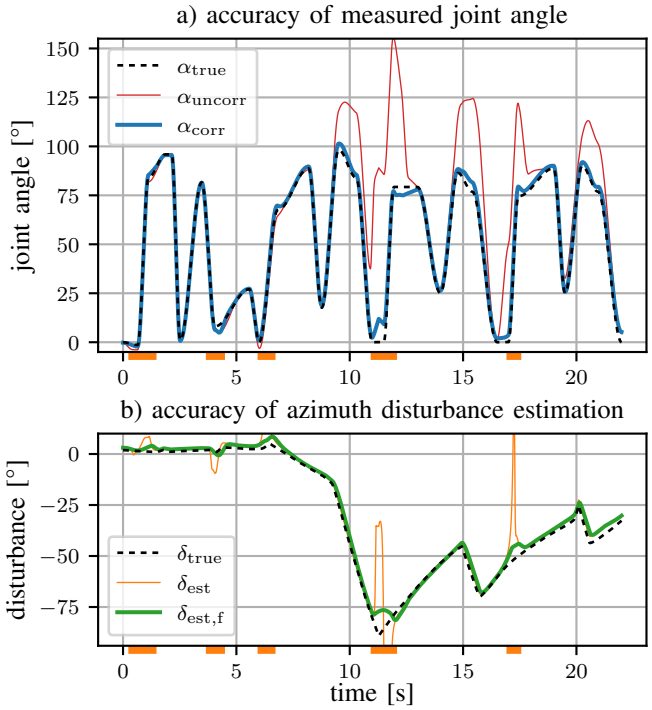

Fig. 6. Joint angles and heading errors for a simulation with a strong magnetic disturbance. a) True (α_true), uncorrected (α_uncorr) and corrected (α_corr) joint angle. b) True (δ_true), unfiltered (δ_est) and filtered ($\delta_\mathrm{est,f}$) estimated heading error. Orange bars mark time periods in which the joint axis is near vertical ($< 10°$).

the calibration. We consider a large number of different combinations of possible sensor-to-segment errors, for each of which both sensor orientations are rotated by random angles around random axes. To quantify the overall magnitude of the modeled error, denote the absolute sum of these rotation angles by E_S.

b) Joint constraint violation: Biological joints such as the knee joint or the interphalangeal joints are only approximate hinge joints and allow for small rotations around other axes. Therefore, we introduce additional rotations around the second and third axis[5] of the joint. Both angles are modeled as sinusoids with random amplitude and phase. To quantify the overall magnitude of the modeled error, denote the absolute sum of both amplitudes by E_J.

Again, for each parameter value, 100 simulation runs are evaluated. The results are shown in Fig. 7. On average, an additional error of $E_\mathrm{S} = 5.0°$ in the sensor-to-segment orientation raises the RMSE from 2.6° to 4.5°. Likewise, the RMSE increases from 2.6° to 3.8° when we relax the hinge joint assumption and allow for rotations around the second and third joint axis with an amplitude sum of $E_\mathrm{J} = 5.0°$.

Note that the effect of the error depends on the axis, which

[5]Without loss of generality, we model the joint orientation using z-x'-y'' Euler angles as recommended for finger joints by the ISB [10].

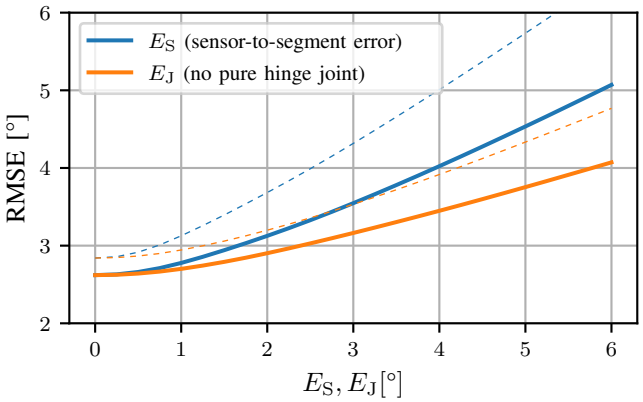

Fig. 7. Sensitivity of the RMSE of the heading-corrected joint angles to errors in the IMU attachment E_S and joint rotations around other axes E_J. Dashed lines indicate mean + standard deviation.

is chosen randomly for both errors. This explains that the standard deviation increases significantly when simulating joint rotation and sensor attachment errors.

Finally, comparing the simulation results for small (finger) motions and large (leg) motions did not yield any notable differences. The error with magnetic disturbance and heading correction slightly increased from 2.6° to 2.9°, but overall, the presented results are equally valid for both cases.

IV. DISCUSSION AND CONCLUSIONS

We proposed and investigated a quaternion-based method to calculate joint angles for approximate hinge joints in non-homogeneous magnetic fields. The method exploits the kinematic constraint of the joint to compensate heading errors caused by the magnetic disturbance. Our results indicate that the method is highly useful in the presence of ferromagnetic material or other magnetic disturbances.

As the posed angle measurement problem becomes singular when the joint axis becomes vertical, a filter was designed that allows accurate tracking for a temporarily vertical joint axis. In the practically less relevant case of a permanently vertical joint axis, additional (non-inertial) sensors are required that overcome the bias-disturbance dilemma of IMUs.

The results show that the method still gives good results when the ideal conditions of a perfect hinge joint and a perfect sensor-to-segment calibration are not met. Finally, the results indicate that the dimensions of the segments and the motion volume hardly influence the accuracy of the method. Therefore, applications include but are not limited to mechanical joints in robotics and approximate hinge joints of the human body such as the knee joint or the interphalangeal joints of the finger. The method is realtime in the sense that only current and previous information is used. It is therefore highly suitable for rehabilitation applications including realtime visualization of motions and feedback control of rehabilitation robotics or functional electrical stimulation systems.

With respect to many other approaches, there are two aspects worth discussing: The first is that the method we propose does not use the IMU measurement data but its estimated orientation. It therefore renders motion analysis more modular and allows for a distributed implementation with sensor fusion on the IMUs and reduced computational effort on the (central) processing unit that determines the joint angle. Finally, note that the method is even suitable for the case in which no magnetometers are employed at all.

The second aspect is that the proposed method does not calculate the joint angle directly but explicitly determines the heading error that is induced by the magnetic inhomogeneity. This proved useful for singularity treatment and will allow us to further extend the method, for example by error source modeling. Likewise, adjusting the orientation quaternions instead of directly calculating joint angles allows the adjusted quaternions to be used for other means, e.g. to implement 3D visualization.

Future research will focus on experimental evaluation of the proposed method as well as extending the method for joints with multiple degrees of freedom.

ACKNOWLEDGMENT

We kindly thank Moritz Apel for his valuable contribution to the experimental recording of the magnetic disturbance.

REFERENCES

[1] J. Diebel, "Representing attitude: Euler angles, unit quaternions, and rotation vectors," *Matrix*, vol. 58, no. 15-16, pp. 1–35, 2006.
[2] W. De Vries, H. Veeger, C. Baten, and F. Van Der Helm, "Magnetic distortion in motion labs, implications for validating inertial magnetic sensors," *Gait & posture*, vol. 29, no. 4, pp. 535–541, 2009.
[3] T. Seel and S. Ruppin, "Eliminating the effect of magnetic disturbances on the inclination estimates of inertial sensors," in *Proc. of 20th IFAC World Congress (to appear in IFAC-PapersOnLine)*, 2017.
[4] T. Seel, J. Raisch, and T. Schauer, "IMU-based joint angle measurement for gait analysis," *Sensors*, vol. 14, no. 4, pp. 6891–6909, 2014.
[5] M. Valtin, C. Salchow, T. Seel, D. Laidig, and T. Schauer, "Modular finger and hand motion capturing system based on inertial and magnetic sensors," *Current Directions in Biomedical Engineering*, vol. 3, no. 1, p. 19–23, 2017.
[6] T. Seel, T. Schauer, and J. Raisch, "Joint axis and position estimation from inertial measurement data by exploiting kinematic constraints," in *Control Applications (CCA), 2012 IEEE International Conference on*. IEEE, 2012, pp. 45–49.
[7] G. Cooper, I. Sheret, L. McMillian, K. Siliverdis, N. Sha, D. Hodgins, L. Kenney, and D. Howard, "Inertial sensor-based knee flexion/extension angle estimation," *Journal of biomechanics*, vol. 42, no. 16, pp. 2678–2685, 2009.
[8] H. G. Kortier, V. I. Sluiter, D. Roetenberg, and P. H. Veltink, "Assessment of hand kinematics using inertial and magnetic sensors," *J Neuroeng Rehabil*, vol. 11, no. 1, p. 70, 2014.
[9] M. Kok, J. D. Hol, and T. B. Schön, "An optimization-based approach to human body motion capture using inertial sensors," *IFAC Proceedings Volumes*, vol. 47, no. 3, pp. 79–85, 2014.
[10] G. Wu, F. C. Van der Helm, H. D. Veeger, M. Makhsous, P. Van Roy, C. Anglin, J. Nagels, A. R. Karduna, K. McQuade, X. Wang, *et al.*, "ISB recommendation on definitions of joint coordinate systems of various joints for the reporting of human joint motion—part II: shoulder, elbow, wrist and hand," *Journal of biomechanics*, vol. 38, no. 5, pp. 981–992, 2005.
[11] Supporting material. [Online]. Available: http://www.control.tu-berlin.de/Hinge_Joint_Constraints